Title: Interplay between Mitochondria and Diet Mediates Pathogen and Stress Resistance in *C. elegans*

Authors: Alexey V. Revtovich[1], Ryan Lee[1], Natalia V. Kirienko[1*]

Affiliations: [1]Department of BioSciences, Rice University, Houston TX, 77005, USA

*** Correspondence:** kirienko@rice.edu

Abstract:

Diet is a crucial determinant of organismal biology. Here we demonstrate the dramatic impact of a subtle shift in diet on the ability of *Caenorhabditis elegans* to survive pathogenic or abiotic stress. Interestingly, this shift occurs independently of canonical host defense pathways, arising instead from improvements in mitochondrial health. Using a variety of assays, we reveal that the most common *C. elegans* food source (*E. coli* OP50) results in a vitamin B12 deficiency that compromises mitochondrial homeostasis. Increasing B12 supply by feeding on *E. coli* HT115 or by supplementing bacterial media with methylcobalamin restored mitochondrial function, even if the bacteria were dead. B12 supplementation also efficiently increased host health without adversely affecting lifespan. Our study forges a molecular link between a dietary deficiency (nutrition/microbiota) and a physiological consequence (host sensitivity), using the host-microbiota-diet framework. The ubiquity of B12 deficiency (~10-40% of US adults) highlights the importance of our findings.

Introduction

The diet and microbiota of an organism define its biology as much as its genome. Unfortunately, an avalanche of descriptive studies on model organism microbiomes have yielded very little mechanistic understanding of the relationships that define the host-microbiota-nutrition axis. One explanation for this is that the interplay amongst the three participants is incredibly complex and surprisingly dynamic. For example, the host and microbiota actively shape and, are in turn shaped by, their nutrition. Host genetics and environment determine initial susceptibility to microbial colonization, which will go on to influence all aspects of health. Establishing a mechanistic understanding of these interrelationships is crucial to the life history of an organism.

Caenorhabditis elegans offers a tantalizing system for simplifying these studies without sacrificing the ability to make discoveries that will be a useful starting point for more advanced organisms. At its most reduced form, the host-microbiota-nutrition axis of *C. elegans* can be collapsed to a binary system comprised of only two species, both of which are genetically tractable. As *C. elegans* is a bacteriovore, a single bacterial species can form the diet and the intestinal flora (due to incomplete disruption and digestion of bacterial food, which then colonizes the intestine). Generation of gnotobiotic worms is also simple and inexpensive.

Even this binary system has yielded significant insight regarding interactions between the host and its bacterial counterpart. For example, studies have shown that not only the relative biomacromolecular content of their diet (i.e., lipids, carbohydrates, etc.) but also bacterial metabolites informed the host's biology, including folate [1], nitric oxide [2], and tryptophan [3,4]. Indeed, even the rate of bacterial respiration affected the metabolic state of the host [5].

In this report, we show that differences in bacterial strains drive increased host sensitivity to a variety of stresses, including exposure to *P. aeruginosa*, oxidative stress, or hyperthermia. Through a panel of orthogonal assays, we demonstrated that a diet of *E. coli* strain OP50 causes a chronic vitamin B12 deficiency that perturbs mitochondrial health and function. B12 supplementation,

even in the absence of living bacteria, increased resistance without shortening lifespan. Our findings provide a mechanistic explanation for the link between diet, cellular homeostasis, and organismal health.

Results

A diet of E. coli strain HT115 confers resistance to a variety of stresses in C. elegans

While characterizing a novel *C. elegans-P. aeruginosa* Liquid Killing assay [6,7], we made the unexpected observation that worms reared on *E. coli* HT115 exhibited increased resistance to *P. aeruginosa* compared to worms reared on *E. coli* OP50 (**Fig 1A, B**). This was true even if bacteria lacked the L4440 RNAi vector. Pathogenesis in this assay requires the siderophore pyoverdine, which compromises host metabolism by removing ferric iron [8]. Since exogenous iron strongly limits host killing [7], we tested whether worms reared on HT115 contained more iron, indirectly increasing their resistance to pyoverdine. However, neither a fluorometric iron (III) assay nor mass spectrometric measurement of total iron showed significant diet-dependent differences in host iron concentration (**Fig S1A, B**).

Substitution of *E. coli* OP50 with a variety of other bacterial foods (or UV- or heat-killed OP50) increases *C. elegans'* lifespan [9-12]. These observations are typically interpreted to mean that OP50 is weakly pathogenic to *C. elegans* [13,14]. On this basis, we surveyed basal gene expression levels for downstream effectors of a variety of *C. elegans* immune pathways, including PMK-1/p38, ZIP-2/bZIP, DAF-16/FOXO, FSHR-1/FSH, and SKN-1/Nrf2 [15-20]. Worms reared on OP50 and HT115 had indistinguishable basal levels of expression of downstream innate immune effectors associated with these pathways (**Fig S2**).

Using either the conventional HT115 RNAi strain or an RNAi-competent OP50 derivative [21], we knocked down key defense pathways and assayed sensitivity to *P. aeruginosa* exposure. Although some knockdowns affected the timing of death (e.g. *daf-2(RNAi)* prolonged survival, *daf-16(RNAi)*

hastened death), worms fed HT115 survived longer in each case (**Fig S3**). These data indicate that weak OP50 pathogenicity (if it does exist) is unlikely to underlie the difference in sensitivity to *P. aeruginosa*.

Many defense pathways confer resistance to both abiotic and pathogenic factors. Therefore, we tested whether HT115 increased resistance to abiotic stresses. As anticipated, survival was significantly increased when HT115-fed worms were exposed to the iron-scavenging xenobiotic 1,10-phenanthroline, heat shock, or juglone-induced oxidative stress (**Fig 1C-E**). Increased resistance to pathogens and abiotic stresses is commonly associated with longer lifespan but, to our surprise, feeding HT115 did not extend lifespan (**Fig 1F**).

Transcriptome profiling implicates mitochondrial defects in diet-induced stress sensitivity

To gain an unbiased snapshot of gene expression in worms fed OP50 or HT115, we performed transcriptome profiling. Interestingly, the number of differentially-regulated genes was very small, with only 35 genes upregulated between 2- and 8-fold in HT115 and 22 genes upregulated between 2- and 20-fold in OP50 (**Table S1**). Strikingly, of the latter 22 genes, 12 encoded proteins localized to the mitochondria (**Table 1**). This enrichment was highly significant (p=2.2*10^{-16}), particularly given that the fraction of nuclear genes that encode mitochondrial proteins in *C. elegans* and humans is ~6% and 7% respectively [22,23]. This enrichment was specific to genes upregulated by an OP50 diet; amongst genes expressed at higher levels in HT115-fed worms, only two mitochondrial genes (*acox-2* and T22B7.7) were observed (2/35=5.7%, p=0.9896). These data argue that feeding with OP50 increases expression of mitochondrial genes. Two genes in particular caught our attention: *hsp-60* encodes a mitochondrial chaperone that is constitutively expressed at low levels and is induced when worms are exposed to mitochondria-damaging treatments [24-26]. *acdh-1* encodes a short-chain acyl-CoA dehydrogenase that has been used as an indicator of branched chain amino acids and/or propionyl-CoA, a mitotoxic byproduct of their metabolism [27].

A diet of HT115 improves the vitamin B12 deficiency caused by OP50

Consistent with our microarray results, we observed increased *acdh-1::*GFP expression in OP50-fed worms, whether measured by conventional imaging (**Fig 2A,B**) or by COPAS flow vermimetry (**Fig 2C**). Efficient metabolism of branched chain amino acids and propionyl-CoA requires vitamin B12 [28,29], an essential micronutrient for most organisms, including *C. elegans* and *E. coli*. Based on these results, we hypothesized that a diet of OP50 causes a B12 deficiency that triggers compensatory increases in expression of *acdh-1*::GFP and other mitochondria-related genes.

We attempted to use mass spectrometry to measure S-adenosylcobalamin in worms fed either HT115 or OP50 (or in the bacteria themselves) to obtain quantitative measurements of vitamin B12. Unfortunately, B12 levels for all samples measured were below the detection threshold, even when samples were concentrated (*data not shown*). To circumvent this limitation we used sodium propionate sensitivity as a functional readout of B12 sufficiency. Consistent with other data, a diet of HT115 significantly increased resistance to propionate, indicating that it improves the B12 shortage (**Fig 2D**).

Vitamin B12 deficiency disrupts mitochondrial homeostasis

We hypothesized that the dietary B12 deficiency causes buildup of propionyl-CoA, which would lead to mitochondrial damage. Therefore, we assayed mitochondrial homeostasis in *C. elegans* fed either OP50 or HT115. Under normal conditions, mitochondrial quality control involves constant fission and fusion events that serve to pool healthy, functional mitochondrial content, while damaged material is sequestered for autophagic recycling [30]. Compared to mammals, *C. elegans* mitochondria generally exhibit greater interconnectivity and longer tubular architecture (e.g., disrupting *C. elegans* mitochondrial genes almost always increases fragmentation [31]). We used a *C. elegans* strain expressing a mitochondrially-targeted GFP [26] to assay mitochondrial health after

OP50 or HT115 consumption. Worms fed HT115 demonstrated increased connectivity and less clumping (i.e., punctae) than OP50 (**Fig 2E**), indicating improved mitochondrial health.

Vitamin B12 supplementation improves mitochondrial health

To determine whether we could remedy the B12 limitation, we spiked OP50 growth medium with exogenous methylcobalamin to a final concentration of 0.2 μg/mL. Supplementation dramatically decreased *acdh-1::GFP* fluorescence (**Fig 2A-C**), increased resistance to propionate (**Fig 2D**), and improved mitochondrial network architecture (**Fig 2E**). Combined, these data suggested that methylcobalamin supplementation significantly improved mitochondrial health.

We assayed other metrics of mitochondrial health, including mitochondrial count (**Fig 2F**), membrane potential (**Fig 2G**), production of reactive oxygen species (ROS, **Fig 2H**), and ATP (**Fig 2I**) to verify this conclusion. Interestingly, methylcobalamin supplementation decreased the number of mitochondria while mitochondrial membrane potential remained steady, indicating that the average membrane potential of each mitochondrion was slightly increased by treatment. Methylcobalamin also significantly decreased ROS production, while ATP production decreased only slightly. The most parsimonious explanation for these observations is that a dietary B12 deficiency significantly compromises mitochondrial health and efficiency.

Vitamin B12 deficiency in OP50 diet drives sensitivity to stress

We predicted that the mild mitochondrial dysfunction exhibited by OP50-fed worms may drive their increased sensitivity to stress. We reared worms on OP50 or OP50 supplemented with methylcobalamin (OP50/B12), and tested their resistance to *P. aeruginosa*. We observed a dramatic difference in host survival: virtually all OP50-fed worms were dead by the time OP50/B12-fed worms showed ~10% death (**Fig 3A, B**). Bacterial metabolism of B12 was superfluous for this effect. *C. elegans* fed heat-killed *E. coli* spotted onto plates containing methylcobalamin-

supplemented media also exhibited virtually no *acdh-1*::GFP expression and increased survival when exposed to *P. aeruginosa* (**Figs S4A, 3C**). Next, we examined whether cobalamin was beneficial during exposure to more generic stressors, like hyperthermia. Supplementation again significantly increased *C. elegans* survival (**Fig 3D**).

A growing body of evidence suggests that decreasing mitochondrial activity, either by genetically compromising oxidative phosphorylation or by caloric restriction, extends lifespan [32,33]. Since B12 supplementation improves mitochondrial function, we wanted to know whether it may be beneficial during adverse conditions, but would also ultimately shorten lifespan. No significant changes in lifespan were seen in worms receiving a diet supplemented with methylcobalamin (**Fig 3E**).

All of the experiments described above were performed in a *glp-4(bn2ts)* background, which fails to generate a germline and is sterile at non-permissive temperatures. Sterility is necessary to avoid non-specific death in the Liquid-Killing assay. To rule out the possibility that the observed phenotypes were a result of the *glp-4 (bn2)* background, we tested wild-type N2 worms. In every case tested, wild-type worms recapitulated our findings from *glp-4(bn2)* mutants (**Fig 3F-H**).

The E. coli TonB transporter mediates vitamin B12 internalization and subsequent host health

Since *E. coli* is unable to synthesize vitamin B12, it must be imported from the extracellular milieu. As efficient import has been reported to require TonB activity [34,35], we evaluated *acdh-1*::GFP fluorescence in worms fed *tonB* deletion mutants [36]. While *acdh-1*::GFP fluorescence in worms reared on the parental strain (*E. coli* BW25113) was similar to OP50 (**Fig S4B**), *tonB* deletion slightly, but reproducibly, increased GFP level (**Fig S4C**, $p<0.01$). Correspondingly, *tonB* deletion also increased sensitivity to *P. aeruginosa* exposure (**Fig S4D**). As with OP50, supplementation of wild-type BW25113 with methylcobalamin completely abolished *acdh-1*::GFP fluorescence (**Fig S4E**). In contrast, *tonB* mutants showed only partial attenuation of GFP

expression after methylcobalamin supplementation, indicating that the bacteria were unable to efficiently internalize the vitamin (**Fig S4F, G**). One possible explanation for the attenuation in GFP fluorescence that we observed in these mutants is that *E. coli* has a salvage pathway to acquire precursors for B12 biosynthesis [37]. Our observation that *tonB* mutation increases host sensitivity to stress still further (**Fig S4D**) indicates a role for TonB activity in the health of the host.

Discussion

Recently, Leulier and colleagues defined the "nutrient-microbiota-host axis" to incorporate all of these determinants into a single conceptual framework [38]. Our results leverage this idea to connect diverse phenomena into an articulated whole. For example, our data indicate that a dietary deficiency in vitamin B12 deficiency causes mitochondrial defects, likely through the buildup of propionyl-CoA (a known mitochondrial toxin). We also demonstrated that this damage significantly increased sensitivity to a variety of stresses. Our findings provide a mechanistic explanation for clinical observations that patients with methylmalonic or propionic acidemias (either of which can arise from vitamin B12 deficiency) exhibit symptoms that are strikingly similar to those with congenital mitochondrial defects (including poor growth, muscle weakness, and disorders of the liver, kidney, and gastrointestinal and respiratory tracts). It also explains why mice with inactive methylmalonyl-CoA mutase (one of two B12-dependent enzymes) exhibit reduced respiratory chain activity [39]. Vitamin B12 is clearly important for normal cellular stress resistance and healthy aging. Despite this, estimates of deficiency range between 10-40% of the population, with increased prevalence in the elderly [40].

Previous studies from the Walhout lab have linked B12 replete diets (including *Comamonas aquaticus* and *E. coli* HT115) to shortened lifespan [41]. We also saw a small, but statistically significant, decrease in maximum lifespan when *C. elegans* was reared on *E. coli* HT115. Intriguingly, methylcobalamin did not affect the lifespan of worms when it was added to an OP50

diet (**Fig 3E**), suggesting that the improvement in mitochondrial health provided by B12 supplementation can be unlinked from lifespan shortening. Currently, we hypothesize that some other aspect of *Comamonas* and HT115 diets, probably a common metabolite, was responsible for this effect.

Interestingly, even though we started to query the host-microbiota-diet axis with a minimal, binary system (*C. elegans* and *E. coli*), a number of unexpected complexities have arisen. For example, subtle differences in the biology of *C. elegans* reared on OP50 or HT115 have generally been attributed to the differences in their origins (i.e., OP50 was derived from an *E. coli* B strain while HT115 came from *E. coli* K12). However, BW25113 (which also originated from K12) showed *acdh-1*::GFP fluorescence similar to that of OP50. Heat-killed OP50 showed *acdh-1*::GFP fluorescence similar to that of HT115-fed *C. elegans*. These data indicate that *acdh-1*::GFP expression and mitochondrial health poorly correlate with strain origin and are likely to be dynamic, illustrating the subtle nuances that lie along the nutrient/microbiota axis and the dramatic impacts they have on host phenotype.

We also showed that this framework can help identify an important mechanism used by *C. elegans*, and presumably more complex metazoans, to fine-tune their cell metabolism to resist adverse environmental factors (including pathogens, heat, and toxins), even without activating canonical host defense pathways. Interestingly, the sensitivity to stress caused by B12 deficiency seems to correlate with the degree of mitochondrial involvement in the stress-induced pathology. For example, we observed that methylcobalamin supplementation decreased *acdh-1* expression by 10-fold or more while proportional increases were seen in resistance to propionate or *P. aeruginosa* in Liquid Killing. This result corroborates our recent findings that place mitochondrial homeostasis at the heart of this pathogenesis model (Tjahjono E, Kirienko N, *personal communication*). Although the effect was smaller, benefits from B12 supplementation were still observed when stresses were more pleiotropic (such as heat shock or oxidative stress, where intracellular contents are more

uniformly damaged). Taken together, our findings emphasize the importance of using a bottom-up approach to effectively understand the mechanisms that connect nutrition, metabolic activity, and the host's microbiota to its health.

Methods

C. elegans strains

All *C. elegans* strains were maintained on nematode growth medium (NGM) seeded with *Escherichia coli* strain OP50, HT115 or BW25113 (see below) with or without supplementation with methylcobalamin at a final concentration of 0.2 mg/L. Worms were reared and passaged at 15˚C [42] unless otherwise noted. For RNAi-mediated gene knockdown, plasmids from the Ahringer library [43] were either used in the HT115(DE3) strain supplied or purified and transformed into an RNAi-competent strain of OP50 (xu363) [21]. All plasmids were sequence verified.

C. elegans strains used in this study included N2 Bristol (wild-type), SS104 [*glp-4*(*bn2*)] [44], NVK44 [*glp-4(bn2); zcIs14*{myo-3::GFP(mt)}], PE327 (ATP reporter): *glp-4(bn2);* feIs5 [sur-5p::luciferase::GFP + rol-6(su1006)] [45], and VL749 [wwIs24{*acdh-1*p::GFP + unc-119(+)}] [41],

Bacterial strains

Bacterial strains used in this study were *E. coli* OP50 and OP50(xu363), *E. coli* HT115(DE3); *E. coli* BW25113, BW25113 *tonB* #1 and BW25113 *tonB* #2 were obtained from Keio Knockout Collection (GE Dharmacon). For pathogenesis assays, *P. aeruginosa* PA14 was used [46].

C. elegans pathogenesis and stress assays

Liquid- and Slow-Killing assays were performed as described elsewhere [47]. Propionate toxicity was measured as described [28]. For oxidative and iron removal stresses, NGM agar plates were supplemented with 120 µM of juglone [48] or 100 µM of phenanthroline, respectively. Heat shock

experiments were carried out at 30 ˚C, lifespan was measured at 25 ˚C. Wild-type *C. elegans* were rendered sterile by *cdc-25.1(RNAi)* when appropriate. For agar-based assays, three plates with 50 worms/plate/strain/biological replicate were used. For liquid-based experiments, 10 wells with 20 worms/well/strain/biological replicate were used. At least three biological replicates were performed for each experiment. Statistical significance was calculated based on log-rank test, except Student's t-test was used for Liquid Killing and propionate toxicity.

Detection of total iron via ICP-MS

For ICP-MS experiments, worms were prepared as for the measurement of internalized pyoverdine. In brief, approximately 24,000 *C. elegans* L1 larvae per sample were raised on NGM plates seeded with *E. coli* strains OP50 or HT115. When they reached young adulthood, they were transferred to 15 mL conicals, washed four times, and then collected with uniform volumes. Samples were frozen, thawed, and disrupted via sonication using a 2 min cycle on a Branson 250 Sonifier set to 70% output, 10% duty cycle. After lysis, samples were transferred to glass scintillation vials and water was evaporated by heating at 100°C on a heating block. Upon the loss of all visible moisture, samples were digested in 4 mL of concentrated, trace-metals grade nitric acid (GFS Chemicals) overnight at 98 °C. For ICP analysis, samples were resuspended in 1 mL concentrated nitric acid, diluted 1/40 into 2% HNO_3 (v:v), 2% ethanol (v:v), and spiked with yttrium/indium as internal standards. For iron quantitation, a seven point calibration curve from 3 ug/L to 200 ug/L was prepared in 2% HNO_3 (v:v), 2% ethanol (v:v) and spiked with yttrium/indium internal standards. Linear correlation coefficients for the iron calibration curve were at least 0.9998.

Quantitation of iron was carried out by inductively-coupled plasma mass spectrometry (ICP-MS) analysis, using a Perkin Elmer Nexion 300X ICP-MS system, operated in the kinetic energy discrimination (KED) mode. Iron was monitored at m/z 57. Yttrium and indium were used as

internal standards and were monitored at m/z 89 and m/z 115, respectively. Quadrupole scanning parameters were set to 20 scans per read, 1 read per replicate, and 3 replicates per sample. The instrument was operated in the peak hopping mode with a dwell time of 50 ms. For KED mode, the cell gas pressure was set at 5, the RPa and RPq were set at 0 and 0.25 respectively. The detector was operated in dual mode. Plasma and auxiliary gas flows were set at 16 and 1.2 L/min respectively. Nebulizer gas flow was tuned at the time of analysis and typically ranged between 0.99 and 1.02 L/min. Plasma power was 1600 W. The peristaltic pump was operated at 20 rpm for analysis and 40 rpm for flushing. Read delay, flush, and wash times were 60, 90 and 120 seconds respectively.

Detection of host ferric iron

Fluorometric determination of ferric iron was performed as follows. First, lysates from young adult *C. elegans*, fed on OP50 or HT115 were prepared as described above. Next, a standard solution of pyoverdine, with fluorescence within linear range of detection by spectrometry (15,000 – 20,000 AU) was prepared. This material was mixed (1:1, v/v) with water, ferric iron, or lysates from *C. elegans*, and incubated for 10 min. Pyoverdine fluorescence was measured using excitation 405 nm, emission 460 nm. As pyoverdine has a 1:1 stoichiometric relationship with iron, the difference between initial and final fluorescence is equivalent to the available ferric iron remaining within *C. elegans*.

Microarray and Quantitative Real-Time PCR (qPCR)

For RNA collection, *glp-4(bn2)* worms were grown on appropriate plates until reaching young adult stage. RNA was purified and hybridized to Affymetrix GeneChips for *C. elegans* at the Partners Center for Personalized Genetic Medicine, Boston, MA, according to manufacturer's protocols. Three biological replicates were tested for each condition. Gene expression was analyzed using

GCRMA (http://www.bioconductor.org). Differentially upregulated genes were determined on the basis of fold change (>2) and the value of modified Wilcoxon rank test >1.5. Wilcoxon coefficient was determined for each probeset as the smallest expression value in the condition with higher average divided by the highest expression value in the condition with lower average. Microarray data were deposited in GEO database and are available using following link: https://www.ncbi.nlm.nih.gov/geo/query/acc.cgi?token=kjibcyuydrstvuj&acc=GSE97678

cDNA synthesis was performed according to manufacturers' protocols (Ambion). qPCR was performed using SYBR Green iQ mix (Bio-Rad). Fold changes were calculated with a ΔΔCt method. Primer sequences are available upon request.

Imaging

For visualization of *myo-3*::GFP(mt) and *acdh-1*::GFP on slides, young adults were grown on appropriate food. Images were acquired and fluorescence was quantified using a Zeiss Axio Imager M2 upright microscope with a Zeiss AxioCam 506 Mono camera and Zen 2 pro (Zeiss) software. Fluorescence was quantified for at least 50 worms per condition per biological replicate. All the fluorescent images were taken under identical exposure conditions. At least three biological replicates were performed. Statistical significance was determined by Student's t-test.

For determination of ATP concentrations, approximately 200 PE327 worms were grown until young adults on OP50 or HT115. The worms were transferred to 96-well, white clear bottom plates and washed in S-basal five times. 150µ Luminescence buffer (0.14M K2PO4, 0.03M sodium citrate, 1% DMSO, 1mM luciferin) was added to each well in the plate (Luz et al., 2016). Bioluminescence and GFP fluorescence was measured kinetically every 5 minutes for 4h using Cytation5 plate reader / imager (BioTek). Luminescence values were normalized to GFP fluorescence.

Flow vermimetry

Flow vermimetry for measurement of *acdh-1*::GFP, MitoTracker Red CMXRos (Invitrogen), or dihydroethidium (Fisher) was performed using COPAS FlowSort as described previously [8]. For each reporter, all the measurements were taken under same settings. At least 2,000 worms/condition/biological replicate were used; at least three biological replicates were performed. Statistical significance was determined by Student's t-test.

Statistical analysis.

For all of the experiments described in the paper at least 3 biological replicates were performed. For Figures 1B-F and 3D, E, and H, statistical significance was determined using a log-rank test (http://bioinf.wehi.edu.au/software/russell/logrank/). For Figures 2B, D, F, G, and H and 3B, C, F, and G, statistical significance was determined using two-tailed Student's t-test. * - $p<0.01$, # - $p<0.05$. For determining enrichment of mitochondrial genes amongst the total pool of genes upregulated in OP50, a *p*-value was calculated using hypergeometric probability distribution. For Supplemental Figures S1-3 and S4 C, D, statistical significance was determined using Student's t-test. * - $p<0.01$. All error bars represent SEM.

References

1 Virk, B. *et al.* Excessive folate synthesis limits lifespan in the C. elegans: E. coli aging model. *BMC biology* **10**, 67, doi:10.1186/1741-7007-10-67 (2012).

2 Gusarov, I. *et al.* Bacterial nitric oxide extends the lifespan of C. elegans. *Cell* **152**, 818-830, doi:10.1016/j.cell.2012.12.043 (2013).

3 Gracida, X. & Eckmann, C. R. Fertility and germline stem cell maintenance under different diets requires nhr-114/HNF4 in C. elegans. *Current biology : CB* **23**, 607-613, doi:10.1016/j.cub.2013.02.034 (2013).

4 Anyanful, A. *et al.* Paralysis and killing of Caenorhabditis elegans by enteropathogenic Escherichia coli requires the bacterial tryptophanase gene. *Molecular microbiology* **57**, 988-1007, doi:10.1111/j.1365-2958.2005.04739.x (2005).

5 Saiki, R. *et al.* Altered bacterial metabolism, not coenzyme Q content, is responsible for the lifespan extension in Caenorhabditis elegans fed an Escherichia coli diet lacking coenzyme Q. *Aging cell* **7**, 291-304, doi:10.1111/j.1474-9726.2008.00378.x (2008).

6 Conery, A. L., Larkins-Ford, J., Ausubel, F. M. & Kirienko, N. V. High-throughput screening for novel anti-infectives using a C. elegans pathogenesis model. *Current protocols in chemical biology* **6**, 25-37, doi:10.1002/9780470559277.ch130160 (2014).

7 Kirienko, N. V. *et al.* Pseudomonas aeruginosa disrupts Caenorhabditis elegans iron homeostasis, causing a hypoxic response and death. *Cell host & microbe* **13**, 406-416, doi:10.1016/j.chom.2013.03.003 (2013).

8 Kirienko, N. V., Ausubel, F. M. & Ruvkun, G. Mitophagy confers resistance to siderophore-mediated killing by Pseudomonas aeruginosa. *Proceedings of the National Academy of Sciences of the United States of America* **112**, 1821-1826, doi:10.1073/pnas.1424954112 (2015).

9 Win, M. T. *et al.* Validated Liquid Culture Monitoring System for Lifespan Extension of Caenorhabditis elegans through Genetic and Dietary Manipulations. *Aging and disease* **4**, 178-185 (2013).

10 Kim, D. H. Bacteria and the aging and longevity of Caenorhabditis elegans. *Annual review of genetics* **47**, 233-246, doi:10.1146/annurev-genet-111212-133352 (2013).

11 Gomez, F. *et al.* Delayed accumulation of intestinal coliform bacteria enhances life span and stress resistance in Caenorhabditis elegans fed respiratory deficient E. coli. *BMC microbiology* **12**, 300, doi:10.1186/1471-2180-12-300 (2012).

12 Yu, L. *et al.* Bacterial Respiration and Growth Rates Affect the Feeding Preferences, Brood Size and Lifespan of Caenorhabditis elegans. *PloS one* **10**, e0134401, doi:10.1371/journal.pone.0134401 (2015).

13 Garsin, D. A. *et al.* A simple model host for identifying Gram-positive virulence factors. *Proceedings of the National Academy of Sciences of the United States of America* **98**, 10892-10897, doi:10.1073/pnas.191378698 (2001).

14 Garigan, D. *et al.* Genetic analysis of tissue aging in Caenorhabditis elegans: a role for heat-shock factor and bacterial proliferation. *Genetics* **161**, 1101-1112 (2002).

15 Papp, D., Csermely, P. & Soti, C. A role for SKN-1/Nrf in pathogen resistance and immunosenescence in Caenorhabditis elegans. *PLoS pathogens* **8**, e1002673, doi:10.1371/journal.ppat.1002673 (2012).

16 Estes, K. A., Dunbar, T. L., Powell, J. R., Ausubel, F. M. & Troemel, E. R. bZIP transcription factor zip-2 mediates an early response to Pseudomonas aeruginosa infection in Caenorhabditis elegans. *Proceedings of the National Academy of Sciences of the United States of America* **107**, 2153-2158, doi:10.1073/pnas.0914643107 (2010).

17 Kim, D. H. *et al.* Integration of Caenorhabditis elegans MAPK pathways mediating immunity and stress resistance by MEK-1 MAPK kinase and VHP-1 MAPK phosphatase. *Proceedings of*

the National Academy of Sciences of the United States of America **101**, 10990-10994, doi:10.1073/pnas.0403546101 (2004).

18 Troemel, E. R. *et al.* p38 MAPK regulates expression of immune response genes and contributes to longevity in C. elegans. *PLoS genetics* **2**, e183, doi:10.1371/journal.pgen.0020183 (2006).

19 Garsin, D. A. *et al.* Long-lived C. elegans daf-2 mutants are resistant to bacterial pathogens. *Science* **300**, 1921, doi:10.1126/science.1080147 (2003).

20 Powell, J. R., Kim, D. H. & Ausubel, F. M. The G protein-coupled receptor FSHR-1 is required for the Caenorhabditis elegans innate immune response. *Proceedings of the National Academy of Sciences of the United States of America* **106**, 2782-2787, doi:10.1073/pnas.0813048106 (2009).

21 Xiao, R. *et al.* RNAi Interrogation of Dietary Modulation of Development, Metabolism, Behavior, and Aging in C. elegans. *Cell reports* **11**, 1123-1133, doi:10.1016/j.celrep.2015.04.024 (2015).

22 Li, J. *et al.* Proteomic analysis of mitochondria from Caenorhabditis elegans. *Proteomics* **9**, 4539-4553, doi:10.1002/pmic.200900101 (2009).

23 Prokisch, H. *et al.* MitoP2: the mitochondrial proteome database--now including mouse data. *Nucleic acids research* **34**, D705-711, doi:10.1093/nar/gkj127 (2006).

24 Yoneda, T. *et al.* Compartment-specific perturbation of protein handling activates genes encoding mitochondrial chaperones. *Journal of cell science* **117**, 4055-4066, doi:10.1242/jcs.01275 (2004).

25 Haynes, C. M., Petrova, K., Benedetti, C., Yang, Y. & Ron, D. ClpP mediates activation of a mitochondrial unfolded protein response in C. elegans. *Developmental cell* **13**, 467-480, doi:10.1016/j.devcel.2007.07.016 (2007).

26 Benedetti, C., Haynes, C. M., Yang, Y., Harding, H. P. & Ron, D. Ubiquitin-like protein 5 positively regulates chaperone gene expression in the mitochondrial unfolded protein response. *Genetics* **174**, 229-239, doi:10.1534/genetics.106.061580 (2006).

27 Schwab, M. A. *et al.* Secondary mitochondrial dysfunction in propionic aciduria: a pathogenic role for endogenous mitochondrial toxins. *The Biochemical journal* **398**, 107-112, doi:10.1042/BJ20060221 (2006).

28 Watson, E. *et al.* Interspecies systems biology uncovers metabolites affecting C. elegans gene expression and life history traits. *Cell* **156**, 759-770, doi:10.1016/j.cell.2014.01.047 (2014).

29 Watson, E., Yilmaz, L. S. & Walhout, A. J. Understanding Metabolic Regulation at a Systems Level: Metabolite Sensing, Mathematical Predictions, and Model Organisms. *Annual review of genetics* **49**, 553-575, doi:10.1146/annurev-genet-112414-055257 (2015).

30 Liesa, M. & Shirihai, O. S. Mitochondrial dynamics in the regulation of nutrient utilization and energy expenditure. *Cell metabolism* **17**, 491-506, doi:10.1016/j.cmet.2013.03.002 (2013).

31 Ichishita, R. *et al.* An RNAi screen for mitochondrial proteins required to maintain the morphology of the organelle in Caenorhabditis elegans. *Journal of biochemistry* **143**, 449-454, doi:10.1093/jb/mvm245 (2008).

32 Yang, W. & Hekimi, S. Two modes of mitochondrial dysfunction lead independently to lifespan extension in Caenorhabditis elegans. *Aging cell* **9**, 433-447, doi:10.1111/j.1474-9726.2010.00571.x (2010).

33 Luz, A. L., Lagido, C., Hirschey, M. D. & Meyer, J. N. In Vivo Determination of Mitochondrial Function Using Luciferase-Expressing Caenorhabditis elegans: Contribution of Oxidative Phosphorylation, Glycolysis, and Fatty Acid Oxidation to Toxicant-Induced Dysfunction. *Current protocols in toxicology* **69**, 25 28 21-25 28 22, doi:10.1002/cptx.10 (2016).

34 Bassford, P. J., Jr., Bradbeer, C., Kadner, R. J. & Schnaitman, C. A. Transport of vitamin B12 in tonB mutants of Escherichia coli. *Journal of bacteriology* **128**, 242-247 (1976).

35 Kadner, R. J. Vitamin B12 transport in Escherichia coli: energy coupling between membranes. *Molecular microbiology* **4**, 2027-2033 (1990).

36 Baba, T. *et al.* Construction of Escherichia coli K-12 in-frame, single-gene knockout mutants: the Keio collection. *Molecular systems biology* **2**, 2006 0008, doi:10.1038/msb4100050 (2006).

37 Fang, H., Kang, J. & Zhang, D. Microbial production of vitamin B12: a review and future perspectives. *Microbial cell factories* **16**, 15, doi:10.1186/s12934-017-0631-y (2017).

38 Leulier, F. *et al.* Integrative Physiology: At the Crossroads of Nutrition, Microbiota, Animal Physiology, and Human Health. *Cell metabolism* **25**, 522-534, doi:10.1016/j.cmet.2017.02.001 (2017).

39 Chandler, R. J. *et al.* Mitochondrial dysfunction in mut methylmalonic acidemia. *FASEB journal : official publication of the Federation of American Societies for Experimental Biology* **23**, 1252-1261, doi:10.1096/fj.08-121848 (2009).

40 Spence, J. D. Metabolic vitamin B12 deficiency: a missed opportunity to prevent dementia and stroke. *Nutrition research* **36**, 109-116, doi:10.1016/j.nutres.2015.10.003 (2016).

41 MacNeil, L. T., Watson, E., Arda, H. E., Zhu, L. J. & Walhout, A. J. Diet-induced developmental acceleration independent of TOR and insulin in C. elegans. *Cell* **153**, 240-252, doi:10.1016/j.cell.2013.02.049 (2013).

42 Stiernagle, T. Maintenance of C. elegans. *WormBook : the online review of C. elegans biology*, 1-11, doi:10.1895/wormbook.1.101.1 (2006).

43 Kamath, R. S. *et al.* Systematic functional analysis of the Caenorhabditis elegans genome using RNAi. *Nature* **421**, 231-237, doi:10.1038/nature01278 (2003).

462 44 Beanan, M. J. & Strome, S. Characterization of a germ-line proliferation mutation in C.
463 elegans. *Development* **116**, 755-766 (1992).
464 45 Luz, A. L., Lagido, C., Hirschey, M. D. & Meyer, J. N. In Vivo Determination of Mitochondrial
465 Function Using Luciferase-Expressing Caenorhabditis elegans: Contribution of Oxidative
466 Phosphorylation, Glycolysis, and Fatty Acid Oxidation to Toxicant-Induced Dysfunction. *Curr*
467 *Protoc Toxicol* **69**, 25.28.21-25.28.22, doi:10.1002/cptx.10 (2016).
468 46 Rahme, L. G. *et al.* Common virulence factors for bacterial pathogenicity in plants and
469 animals. *Science* **268**, 1899-1902 (1995).
470 47 Kirienko, N. V., Cezairliyan, B. O., Ausubel, F. M. & Powell, J. R. Pseudomonas aeruginosa
471 PA14 pathogenesis in Caenorhabditis elegans. *Methods Mol Biol* **1149**, 653-669,
472 doi:10.1007/978-1-4939-0473-0_50 (2014).
473 48 Kirienko, N. V. & Fay, D. S. SLR-2 and JMJC-1 regulate an evolutionarily conserved stress-
474 response network. *The EMBO journal* **29**, 727-739, doi:10.1038/emboj.2009.387 (2010).
475 49 Venkatesan, R. *et al.* Insights into mitochondrial fatty acid synthesis from the structure of
476 heterotetrameric 3-ketoacyl-ACP reductase/3R-hydroxyacyl-CoA dehydrogenase. *Nature*
477 *communications* **5**, 4805, doi:10.1038/ncomms5805 (2014).
478 50 Van Gilst, M. R., Hadjivassiliou, H., Jolly, A. & Yamamoto, K. R. Nuclear hormone receptor
479 NHR-49 controls fat consumption and fatty acid composition in C. elegans. *PLoS biology* **3**,
480 e53, doi:10.1371/journal.pbio.0030053 (2005).
481
482

Acknowledgements

We wish to thank Alex Kang and Dr. Chris Pennington for technical assistance with ICP-MS. *E. coli* OP50(xu363) was provided by Dr Eyleen O'Rourke; some strains were provided by the CGC, which is funded by NIH Office of Research Infrastructure Programs (P40 OD010440). This study was supported by the Cancer Prevention and Research Institute of Texas (CPRIT) RR150044 and National Institutes of Health K22 AI110552 awarded to NVK.

Author Contributions

AVR, RL, and NVK conceived of and performed experiments. AVR and NK analyzed data and wrote the manuscript. NK edited the manuscript and supervised the work.

Competing financial interests

The authors declare no competing financial interests.

Materials & Correspondence

Materials and correspondence should be addressed to Natalia V. Kirienko, kirienko@rice.edu

Figure Legends

Fig 1. HT115 increases *C. elegans'* resistance to stresses. (**A**) Representative brightfield (top) and fluorescent (bottom) images of *C. elegans* exposed to *P. aeruginosa* after feeding on OP50 or HT115. Sytox Orange, a cell-impermeant, fluorescent dye was used to mark dead worms. (**B**) Time course of quantification of staining for conditions in (**A**). (**C-E**) Survival of OP50- and HT115-fed worms after exposure to thermal and oxidative stressors, and acute iron removal. (**F**) Lifespan of *C. elegans* fed with OP50 or HT115. *p*-value for (**B-E**) <0.01, (**F**) – n.s.

Fig 2. HT115 or methylcobalamin supplementation improve mitochondrial health. (**A-C**) Visualization and quantification of *acdh-1*::GFP reporter fluorescence in worms fed various diets, as indicated. (**D-E**) Effect of the diet on propionate toxicity (**D**) and connectivity of mitochondrial network (**E**). (**F-I**) Impact of methylcobalamin (B12) supplementation on mitochondrial count (**F**), membrane potential (**G**), and ROS (**H**) or ATP (**I**) production. * - $p<0.01$, # - $p<0.05$

Fig 3. Methylcobalamin supplementation increases resistance to stress. (**A-B**) Representative images and quantification of *C. elegans* exposed to *P. aeruginosa* after feeding on OP50 with or without methylcobalamin (B12) supplementation. Fraction of dead worms here and elsewhere (1 corresponds to 100% dead) was inferred based on staining with Sytox Orange, a cell impermeant dye. (**C**) Relative death of *C. elegans*, grown on NGM or NGM/methylcobalamin plates with heat-killed OP50 as food source, after exposure to *P. aeruginosa*. (**D-E**) Effect of methylcobalamin-supplemented OP50 feeding on *C. elegans* resistance to heat shock ($p<0.01$) or lifespan ($p>0.05$). (**F-H**) Survival of wild-type worms fed OP50 with or without methylcobalamin supplementation after exposure to *P. aeruginosa* (**F**), propionate (**G**), or hyperthermia (**H**). * - $p<0.01$ (**B, C, F, G**), for (**D, H**), $p<0.01$.

524 **Table 1. Mitochondrial genes upregulated by feeding on *E. coli* OP50**

Gene	Name	Evidence
C05C10.3		Ortholog of human mitochondrial CoA transferase (NP_000427.1); in *C. elegans* mitochondrial proteome [22]
C55B7.4	*acdh-1*	Ortholog to human mitochondrial short chain specific acyl-CoA dehydrogenase (NP_001600.1); responds to propionate level in *C. elegans* mitochondria [41]; in *C. elegans* mitochondrial proteome [22]
F09E10.3	*dhs-25*	Ortholog of mitochondrial dehydrogenase (NP_055049.1) [49]; in *C. elegans* mitochondrial proteome [22]
F09F7.4	*hach-1*	Ortholog of human mitochondrial CoA hydrolase (NP_055177.2), in *C. elegans* mitochondrial proteome [22]
F22B8.7		Ortholog of human mitochondrial amidoxime reducing component (NP_073583.3), in *C. elegans* mitochondrial proteome [22]
F28F8.2	*acs-2*	Ortholog of human mitochondrial acyl-CoA synthetase (NP_079425.3), localized to mitochondria [50]; in *C. elegans* mitochondrial proteome [22]
F32D8.12		Ortholog of human mitochondrial lactate dehydrogenase (NP_705690.2); in *C. elegans* mitochondrial proteome [22]
F37B4.7	*folt-2*	In *C. elegans* mitochondrial proteome [22]
F44G3.2	*argk-1*	Ortholog of human mitochondrial creatine kinase (NP_001814)
F54D5.12		Ortholog of human mitochondrial hydroxyglutarate dehydrogenase (NP_689996.4), in *C. elegans* mitochondrial proteome [22]
Y22D7AL.5	*hsp-60*	Mitochondrial heat shock protein [24]; in *C. elegans* mitochondrial proteome [22]
Y38F1A.6	*hphd-1*	Ortholog of human mitochondrial hydroxyacid-oxoacid transhydrogenase (NP_653251.2), in *C. elegans* mitochondrial proteome [22]

525

526

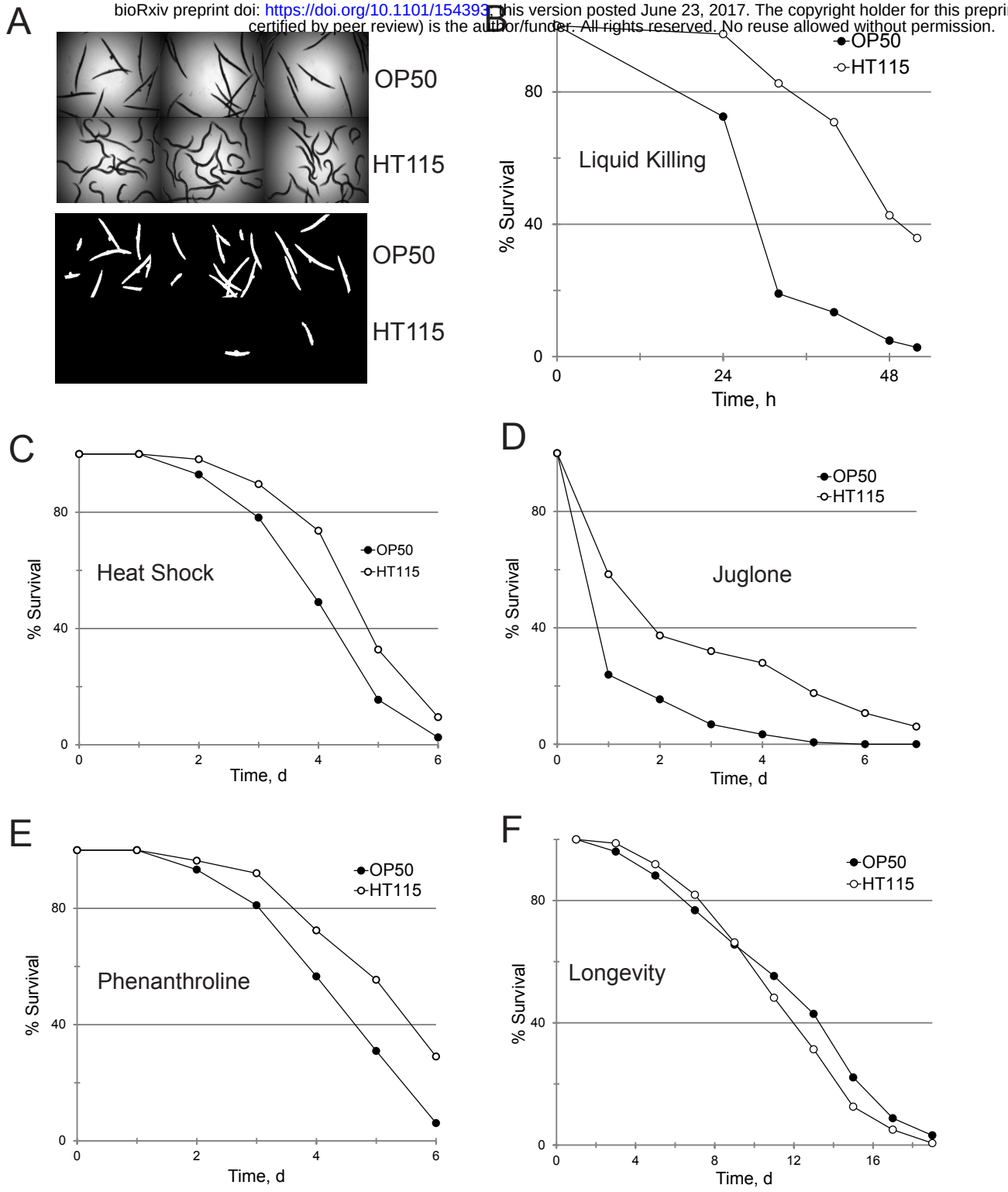

Figure 1

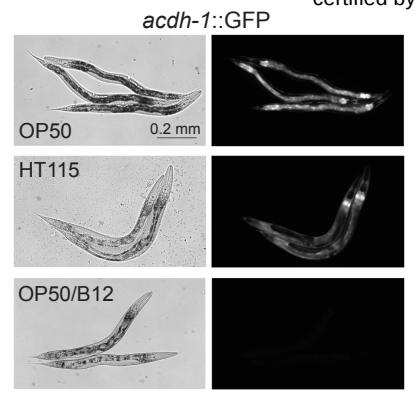

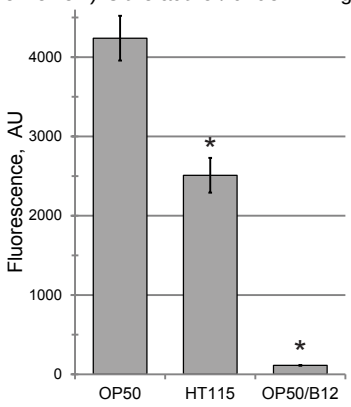

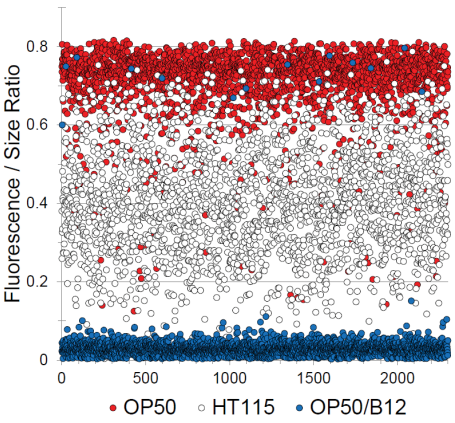

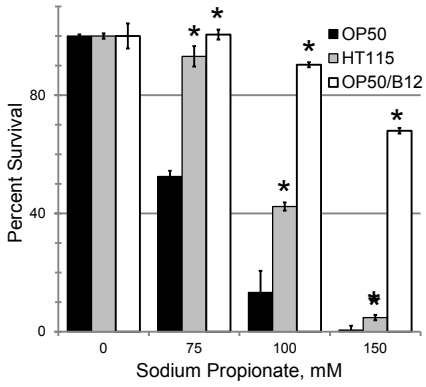

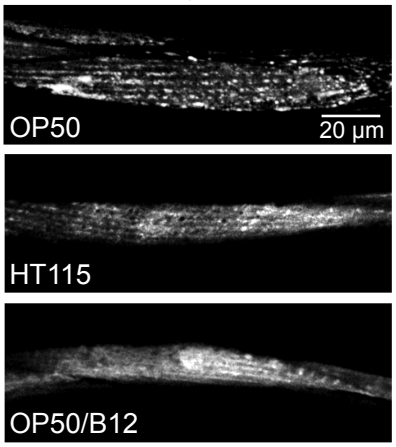

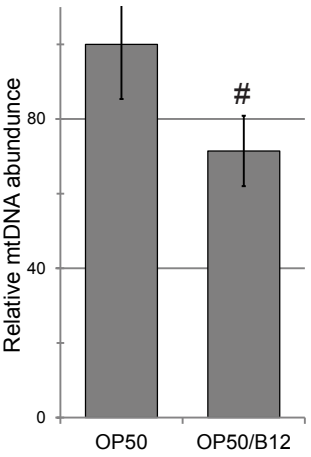

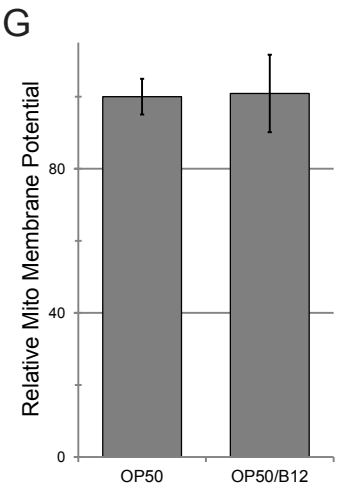

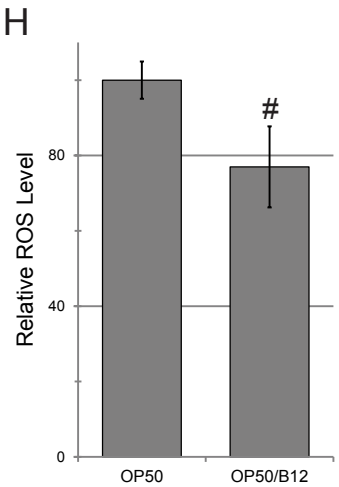

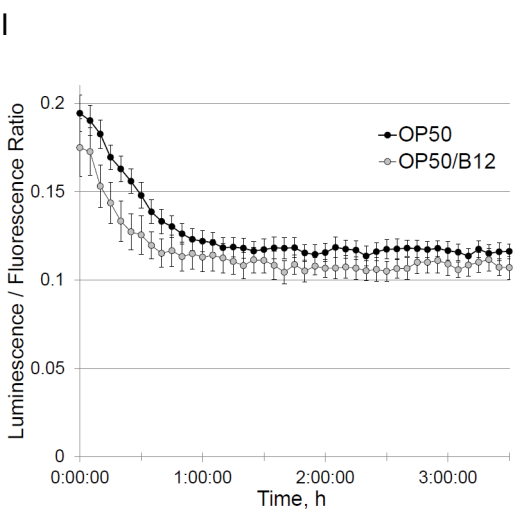

Figure 2

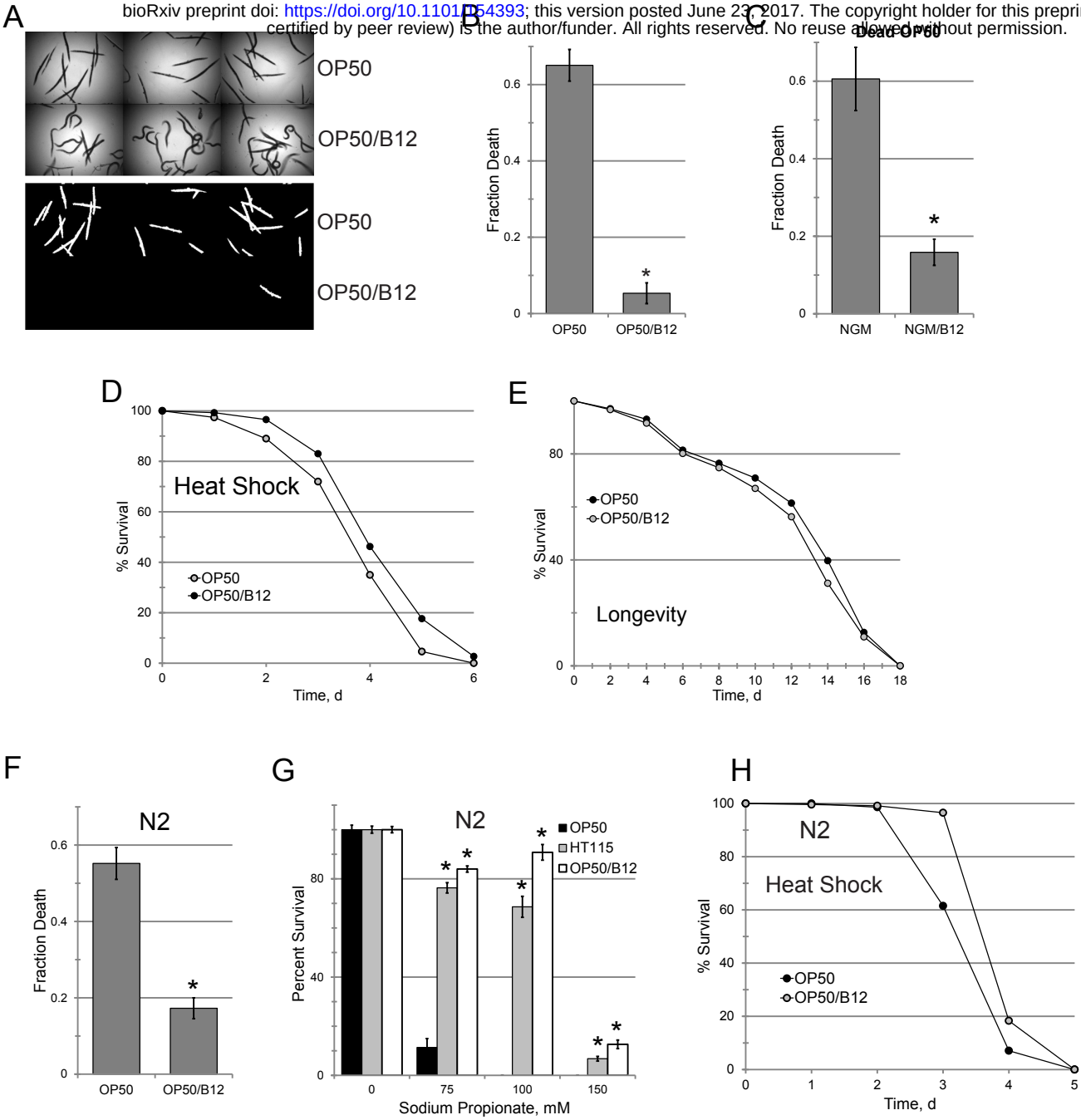

Figure 3